HHS Public Access

Author manuscript

Oncogene. Author manuscript; available in PMC 2016 August 20.

Published in final edited form as:

Oncogene. 2015 August 20; 34(34): 4448–4459. doi:10.1038/onc.2014.372.

A stress-induced early innate response causes multidrug tolerance in melanoma

D Ravindran Menon[1,2,3], **S Das**[4], **C Krepler**[5], **A Vultur**[5], **B Rinner**[2], **S Schauer**[4], **K Kashofer**[4], **K Wagner**[2], **G Zhang**[5], **E Bonyadi Rad**[1,2], **NK Haass**[6], **HP Soyer**[3,6], **B Gabrielli**[6], **R Somasundaram**[5], **G Hoefler**[4], **M Herlyn**[5], and **H Schaider**[1,2,3,6]

[1]Cancer Biology Unit, Department of Dermatology, Medical University of Graz, Graz, Austria

[2]Center for Medical Research, Medical University of Graz, Graz, Austria

[3]Dermatology Research Centre, Translational Research Institute, School of Medicine, The University of Queensland, Brisbane, Queensland, Australia

[4]Institute of Pathology, Medical University of Graz, Graz, Austria

[5]The Wistar Institute, Philadelphia, PA, USA

[6]The University of Queensland, The University of Queensland Diamantina Institute, Translational Research Institute, Brisbane, Australia.

Abstract

Acquired drug resistance constitutes a major challenge for effective cancer therapies with melanoma being no exception. The dynamics leading to permanent resistance are poorly understood but are important to design better treatments. Here we show that drug exposure, hypoxia or nutrient starvation leads to an early innate cell response in melanoma cells resulting in multidrug resistance, termed induced drug-tolerant cells (IDTCs). Transition into the IDTC state seems to be an inherent stress reaction for survival toward unfavorable environmental conditions or drug exposure. The response comprises chromatin remodeling, activation of signaling cascades and markers implicated in cancer stemness with higher angiogenic potential and tumorigenicity. These changes are characterized by a common increase in CD271 expression concomitantly with loss of differentiation markers such as melan-A and tyrosinase, enhanced aldehyde dehydrogenase (ALDH) activity and upregulation of histone demethylases. Accordingly, IDTCs show a loss of H3K4me3, H3K27me3 and gain of H3K9me3 suggesting activation and repression of differential genes. Drug holidays at the IDTC state allow for reversion into parental cells re-sensitizing them to the drug they were primarily exposed to. However, upon continuous drug exposure IDTCs eventually transform into permanent and irreversible drug-resistant cells. Knockdown of CD271 or KDM5B decreases transition into the IDTC state substantially but does not prevent it. Targeting

Correspondence: Dr H Schaider, Dermatology Research Centre, Translational Research Institute, School of Medicine, The University of Queensland, 37 Kent Street, Woolloongabba, Queensland 4102, Australia. h.schaider@uq.edu.au.

CONFLICT OF INTEREST

The authors declare no conflicts of interest.

Supplementary Information accompanies this paper on the Oncogene website (http://www.nature.com/onc)

IDTCs would be crucial for sustainable disease management and prevention of acquired drug resistance.

INTRODUCTION

Over decades of research and development, acquired drug resistance has always been a major challenge for cancer treatment. The advent of molecular targeted therapies provides improved and less toxic options, whereupon generic drugs were replaced by more specific therapeutic inhibitors. This approach showed promising results in multiple cancers including BRAF-mutated melanomas.[1] Acquired drug resistance, however, remains a major obstacle[2] in the path of sustainable disease management or long-term survival.

Opposed to earlier models of permanent drug resistance, recent studies have suggested that phenotypic plasticity is a key factor to the emergence of a transient drug-resistant state, which is reversible in nature by timely drug holidays[3,4] exemplified in the case of BRAF inhibitors. It is unknown whether phenotypic plasticity is due to selection of a subpopulation of cells as described by various reports[4–6] or whether it could be a generic stress-induced response of melanoma cells to a stressful environment.

In this study we tested whether melanoma cells are capable of exhibiting a generic stress response that could explain the phenotypic plasticity contributing to drug resistance. While approaching this question we observed that melanoma cells are capable of exhibiting an early innate response to stressful environments. This innate response not only allows cells to exert multidrug tolerance, but in addition provides them with highly tumorigenic properties. On continuous drug exposure IDTCs experience transition into permanent drug resistance reversing into a parental cell-like state.

RESULTS

Exposure of melanoma cells to sublethal drug concentrations leads to multidrug tolerance

An increasing amount of literature in cancer biology suggests that drug-resistant subpopulations exist in parental cells and are selected during treatment. If this paradigm holds true, a small group of cells should consistently survive the exposure to different drugs. To test this hypothesis, we exposed 1×10^6 mutant BRAF WM164 metastatic melanoma cells to various concentrations of the BRAF inhibitor PLX4032 (250 nM, 500 nM, 1 and 10 μM) for a period of 12 days. The surviving number of cells calculated in relation to the absolute number of cells seeded at the beginning ranged from 4.51% (±0.35) at 10 μM to 99.5% (±1.48) and 156.5% (±13.43) at 500 and 250 nM, respectively, indicating that at 250 and 500 nM of PLX4032 no significant selection pressure was exerted on the parental population (Figures 1a and b). On the basis of the small number of cells surviving 10 μM PLX4032 we argued that if only a small number of cells were resistant to PLX4032, then the majority of cells surviving lower concentrations of PLX4032 should be eliminated if exposed to higher concentrations of the drug. Therefore, WM164 cells exposed to 250 or 500 nM of PLX4032 for 12 days were exposed to 10 μM PLX4032 for additional 12 days. Contrary to what might be expected, cells exposed to low concentrations of PLX4032

became tolerant toward the higher concentration of the drug. The entire cell population survived the exposure to 10 μM and no significant increase in cell death was observed (Figures 1a and b). This suggests that low and moderate drug concentrations initiate an early adaptive response in the surviving cell population, which subsequently confers tolerance to higher drug concentrations. Real-time cell cycle imaging using WM164-FUCCI cells (Haass *et al*.)[7] suggested an almost complete G1 arrest at concentrations from 500 nM on after 12 h of drug exposure pointing to an immediate growth inhibition that continued for 12 days indicating that no particular outgrowth of any subpopulation occurred (Supplementary Figure S1). Melanoma cells undergoing this early adaptive response were termed 'induced drug-tolerant cells' (IDTCs).

We then determined whether the exhibited drug tolerance of IDTCs was specific for PLX4032 or applicable to other drugs as well. IDTCs generated within 12 days from 250 and 500 nM PLX4032 WM164 cells were further exposed to the MEK inhibitor GSK1120212 (50 nM) or cisplatin (30 μM) for 2 days. The IDTCs showed an even significantly lower sensitivity to the second drug, suggesting that a multidrug tolerant state is achieved within the first 12 days (Figure 1c). This experiment was repeated with the BRAF-mutated A375 malignant melanoma cell line at 100 and 250 nM PLX4032, for which similar results were obtained (Figures 1d and e). Interestingly, a 7-day drug holiday was sufficient to re-sensitize the cells to both PLX4032 and GSK1120212 (Figure 1f). This suggests a drug-induced transition and reversible resistance rather than selection of a preexisting population. Cells surviving high concentrations of PLX4032 also showed similar characteristics (data not shown).

Characterization of IDTCs

To understand the drug tolerance to PLX4032 exhibited by IDTCs, western blot analyses of the key melanoma survival pathways MAPK-ERK and AKT were carried out. WM164 IDTCs showed highly active ERK, MEK and AKT signaling (Figure 2a). Time point analyses monitoring the transition of WM164 to IDTCs following exposure to 500 nM PLX4032 revealed that both phosphorylated AKT and MEK-ERK activation occurred on day 8 after exposure, which further peaked on day 12 (Supplementary Figure S2A). IDTCs were subjected to whole-genome-wide gene expression analysis and expression profiles were compared with the parental population. Substantial differences in global gene expression between WM164 parental and IDTCs were observed (Supplementary Figure S2B). For example, a significant increase in expression of various melanocyte progenitor and proposed melanoma stem cell markers such as CD271 and SOX10[8] along with CD44, SOX2, and the EMT inducer SOX4[9] was observed in IDTCs. They also showed increased expression of various drug efflux genes such as *ABCB5*,[10] *ABCA5*,[11] *ABCB8*[12] and *ABCB4*[13] (Supplementary Figure S2C, Supplementary Table 1A). WM164 IDTCs generated *et al* also showed a loss of differentiation markers such as melan-A[14] and tyrosinase[15] (Figure 2b) suggesting that exposure to stress is inducing an undifferentiated state.

High expression of CD271 was confirmed by flow cytometry in 500 nM PLX4032-generated IDTCs compared with parental cells (Figure 2c). Expression levels of CD271 correlated with drug concentration and time of exposure (Supplementary Figure S2D). Drug-induced

CD271 expression was verified in multiple melanoma cell lines exposed to different drugs including chemotherapy like cisplatin strongly supporting the idea of a generic phenomenon (Supplementary Figures S2E and H). In addition, we observed that CD271+ve IDTCs originate from different subpopulations of parental cells under drug exposure and subsequent drug holidays lead to loss of CD271 expression (Supplementary Figures S3A and E). WM164 IDTCs also exhibited an increase in ALDH activity, which is another proposed marker for cancer stemness[16,17] (Figure 2d). The increase in ALDH activity was confirmed in A375 IDTCs (Supplementary Figure S2I). We then determined whether the IDTC state also encompasses an altered chromatin state. Microarray analyses revealed the upregulation of genes linked to epigenetic remodeling, particularly the H3K27 (*KDM6A*, *KDM6B*) and H3K4 (*KDM1B*, *KDM5A*, *KDM5B*) demethylases (Supplementary Table 1B, Supplementary Figure S2J). Both loss of H3K4me3 and an increase in H3K4 demethylases have been previously reported to induce multidrug tolerance in cancer. In melanoma, the H3K4-demethylating enzyme KDM5B in particular has been demonstrated to be a key marker for a slow cycling subpopulation contributing to drug tolerance.[5,6] In order to assess the activity of this marker, a KDM5B promoter construct tagged to Ds red was employed in WM164 melanoma cells. WM164 IDTCs carrying the Ds red construct showed a high level of activity compared with the parental cells (Supplementary Figure S2K). Accordingly, analyses of H3K4 and H3K27 methylation revealed a downregulation of H3K4me3 and H3K27me3 in IDTCs, whereas there was an increase in H3K9me3 (Figure 2e). The global chromatin modification with loss of H3K4me3 and a gain of H3K9me3 has been associated with transcriptional silencing[18,19] and pathway analysis of microarray data confirmed a downregulation of transcription and replication pathways (Supplementary Figure S4A,B) in the IDTC population, suggesting a slow cycling semiquiescent state. Altogether, our results point to a state of chromatin remodeling guiding cells to an undifferentiated state as a characteristic of the IDTC transition.

To test whether the increase in CD271 might also be observed *in vivo*, xenograft tumors in SCID mice previously induced by subcutaneous injection of BRAF-mutant 451Lu melanoma cells were treated with a low dose (30 mg/kg) of PLX4720 (BRAF inhibitor). The dosage did not substantially influence tumor growth (Figure 2f). Tumors harvested following 2 weeks of low-dose treatment showed an increase in CD271 expression, suggesting a transition to the IDTC state similar to what was observed *et al* (Figure 2f). Further investigations in two matched patient samples pre- and post therapy with either vemurafenib or chemotherapy showed increased numbers of CD271+ve cells after treatment, with the majority of CD271+ve cells being located in close proximity to tumor blood vessels (Figure 2g).

IDTCs show high angiogenic and tumorigenic properties

To test for functional characteristics of WM164, IDTCs parental cells and IDTCs were plated at 50, 500 and 5000 cells/well in ultralow attachment plates without drug exposure for a period of 7 days, to probe for their capability to form spheroids. IDTCs but not parental cells grew as melanoma spheroids at a significantly higher rate, even when plated at 50 cells per well, for which parental cells failed to initiate spheroid formation (Figure 3a). On the basis of these observations we tested the tumorigenic potential of IDTCs *in vivo* using a

xenograft NOD.CB17-Prkdcscid/J mouse model by injecting 50, 500 and 5000 cells per site of either WM164 IDTCS or parental cells. Palpable tumors at IDTC-injected sites were observed within 20 days for both 500 and 5000 cells, whereas tumor development was delayed by more than a week at the sites where parental cells were injected (Figure 3b). Tumor volumes from parental cells were also found to be significantly lower than for IDTC-generated tumors especially when injected at a low cell number. These results suggest that IDTCs have an enhanced tumorigenic potential under drug-free conditions. The high tumorigenic property of IDTCs prompted us to investigate the angiogenic signature. Conditioned medium from parental cells and IDTCs was probed for multiple angiogenic factors using an angiogenesis array. IDTCs secreted high levels of angiogenin, angiopoietin1, angiopoietin2, artemin, epidermal growth factor (EGF), endocrine gland derived vascular endothelial growth factor (EG-VEGF), hepatocyte growth factor (HGF) and insulin-like growth factor binding protein 2 (IGFBP2) (Figure 3c). These *et al* results were corroborated by staining tumor tissue from our xenografts with CD31, to detect vessel formation. IDTC tumors showed increased vessel formation compared with parental tumors (Figure 3d) indicating that the expression of angiogenic factors by IDTCs leads to increased vascularization. Together, the studies indicate that the transition of parental cells to IDTCs is accompanied by an increased angiogenic potential further supporting the occurrence of increased tumorigenicity.

Exposure to stress-inducing environments such as hypoxia or nutrient starvation generates an IDTC-like phenotype

The formation of IDTCs based on exposure to different drugs made us ponder whether environmental factors usually present in the tumor microenvironment, such as hypoxia or nutrient starvation, might also instigate their formation. WM164 cells were exposed to moderate (5% O_2) or pronounced hypoxic (1% O_2) conditions for a period of 12 days. At 1% O_2 significant cell death was observed (survival percentage 36.5 (±3.74) %), corresponding to high concentrations of PLX4032, but no reduction in the number of viable cells was found at 5% O_2 (122.5 (±9.1) %; Figure 4a). Equivalent to drug exposure, moderate hypoxic conditions evoked tolerance toward exposure to 1% O_2 mimicking an IDTC state. The experiments were repeated under glucose-starving conditions, whereupon WM164 cells were subjected to low glucose at 1 mg/ml or no glucose media for a period of 12 days. In the absence of glucose the entire parental population died within 12 days, whereas at 1 mg/ml most of the cells survived (95.15 (±1.9) %). In addition, cells surviving the low-glucose condition were found to be tolerant if immediately switched to no glucose media over 12 days (Figure 4b). The cells surviving moderate hypoxia and low glucose were probed for characteristics observed in drug-induced IDTCs. An increase in CD271 expression and ALDH activity was observed in WM164 cells exposed to both conditions (Figures 4c and d). A375 cells exposed to 5% O_2 also showed an increase in CD271 and ALDH activity (Supplementary Figure S5A). Reverse transcription–PCR analysis of WM164 hypoxia and low-glucose-exposed cells revealed an increase in ABCB5, the stem cell marker OCT4 and KDM5A expression under both conditions (Supplementary Figure S5B). The expression of other markers seems to be context-dependent, as an increase of KDM5B was only observed under hypoxic conditions and SOX10 only in cells exposed to low glucose (Supplementary Figure S5C). Invariably, both 5% O_2 and lowglucose-exposed

cells displayed increased ERK and AKT phosphorylation (Figure 4e), along with a loss of H3K4me3 and H3K27me3 as well as a gain of H3K9me3 (Figure 4f). The increase in ERK phosphorylation in IDTCs resulting from exposure to a BRAF inhibitor was thought to be a drug-related response bypassing BRAF signaling, as previously reported.[20] Rather, this signaling pattern appears to be the same in cells arising from exposure to hypoxic and low-glucose conditions, suggesting a generic response contributing to ERK activation.

As the expression of specific markers found in drug-induced IDTCs was analogous to cells evolving under hypoxic or lowglucose conditions, we further probed whether these cells exhibit multidrug tolerance by exposing them to PLX4032 (10 μM), GSK1120212 (50 nM) or cisplatin (10 μM; Figure 4g). Low caspase 3 activities were found for cells pre-exposed to hypoxic or lowglucose conditions compared with parental cells, indicating the acquisition of a phenotype conferring tolerance toward multiple drugs. Similar results were obtained in A375 cells exposed to 5% O_2 (Supplementary Figure S5D). These data suggest that an IDTC-like state can be urged by common microenvironmental factors such as hypoxia or low nutrient availability, which points to a general early innate response to persistent hazardous conditions.

CD271 or KDM5B knockdown limits the efficiency of transition into an IDTC state

Previous reports on targeting tolerant subpopulations have suggested combination strategies involving inhibitors of IGF-1R, the AKT pathway or the HDAC inhibitor TSA, eradicating a preexisting slow cycling multidrug-tolerant population.[4] We tested these strategies on PLX4032-induced WM164 IDTCs, as well as on IDTCs from 5% hypoxia and low glucose by exposing these cells to a combination of PLX4032 with OSI906 (IGF-1R inhibitor), Ly294002 (Pi3K/AKT inhibitor) or TSA. Regardless of the treatment combination, IDTCs consistently showed a high tolerance toward treatment when compared with parental cells (Figure 5a). Accordingly, exposure of already established IDTCs over 12 days to the same drug combinations did not result in a notable effect on survival; rather, the combination seemed to induce a minor reduction in growth rate (Supplementary Figure S6A).

These results prompted us to look for alternative approaches to target IDTCs. The increased CD271 expression as a characteristic marker of IDTCs suggested a potential new target that could resensitize cells, similar to what has been reported for KDM5B in eliminating a slow cycling melanoma population.[6] Indeed, stable knockdown of either CD271 (WM164 sh CD271) or KDM5B (WM164 sh KDM5B) in the parental cells increased their sensitivity to single or combination strategies compared with control short hairpin RNA (shRNA)-transduced WM164 cells exposed to single or combined treatments (Figure 5b). More durable effects were observed in the case of prolonged exposure over 12 days to different concentrations of PLX4032, whereupon the number of surviving cells was substantially reduced in WM164 shCD271 and WM164 shKDM5B cells, even at 250 and 500 nM (Figure 5c). Despite the considerable cell death observed in CD271 and KDM5B knockdown cells upon exposure to single or combined drug strategies, the reminiscent population, unexpectedly, invariably displayed drug tolerance similar to that of IDTCs rising from the control shRNA transduced parental cell population (Figure 5d). This was also true for a combination of PLX4032 with oligomycin A, which affects the mitochondrial survival

pathways and has been reported to eradicate slow cycling cells.[6] The expression of CD271 and KDM5B was analyzed in the surviving WM164 shCD271 and WM164 shKDM5B IDTCs to ensure that the results observed were not due to inefficient knockdown of protein or loss of shRNA expression (Supplementary Figures S6B and C). The silencing of KDM5B could favor the occurrence of a presumed subpopulation of tolerant cells lacking KDM5B expression. To test this WM164 shKDM5B-transduced cells were labeled with a Ds red KDM5B promoter. The WM164 shKDM5B IDTCs also showed higher KDM5B promoter activity (Figure 5e), suggesting that no distinct subpopulation of cells that naturally lack KDM5B expression was selected during the process.

Altogether the results suggest that several combined treatment strategies that have been reported so far to eliminate multidrug-tolerant cells cannot fully eradicate the IDTC population, rather they are more effective in increasing cell death in the parental population before transition into IDTCs.

IDTCs activate multiple signaling pathways allowing rewiring of signaling and tolerance to targeted inhibitors

Our observation that IDTCs remain insensitive to multiple drugs, even after targeting the pathways they depend upon, is intriguing. Hence, the impact of drugs in cell signaling was monitored by exposing PLX4032-generated IDTCs to a combination of PLX4032 and GSK1120212, as they showed a high level of MEK phosphorylation. As expected, exposure to GSK1120212 completely inhibited MEK phosphorylation on days 3, 6 and 12 (Figure 6a). However, it was interesting to note that ERK phosphorylation was only partially inhibited by GSK1120212 indicating that ERK phosphorylation is not exclusively wired through MEK phosphorylation in IDTCs. Moreover, GSK1120212-induced downregulation of ERK phosphorylation only lasted for few days since ERK phosphorylation was re-established in IDTCs on day 12 (Figure 6a).

The phenomenon of rewiring in IDTCs subsequently resulting in drug tolerance was tested for PI3K/AKT and HDAC inhibitors as well. To this purpose, IDTCs were exposed to a combination of PLX4032 along with either the PI3K inhibitor Ly294002 or the HDAC inhibitor TSA for a period of 12 days and cells were harvested for analyses on days 3, 6 and 12. When Ly294002 was used in combination with PLX4032, a downregulation of AKT signaling on days 3 and 8 was achieved, but on day 12, a reactivation of signaling was observed (Figure 6b). HDAC inhibitors have been reported to increase H3K4me3 expression levels that has been linked to transcriptional activation of promoters[18] and to decrease H3K9me3[21] a transcriptional repressor.[19] Therefore, expression levels of these two markers after exposure of IDTCs to TSA (100 nM) were determined. On day 3, an increase in H3K4me3 and loss of H3K9me3 was observed, whereas on continuous exposure for 12 days, expression levels of H3K4me3 and H3K9me3 reversed to IDTC levels before exposure to TSA (Figure 6c). These results suggest that IDTCs have a unique capability to rewire through multiple signaling cascades in order to regain their innate IDTC state.

To test for activation of multiple signaling pathways, WM164 parental and IDTC cell lysates were subjected to reverse phase protein array (RPPA) analyses. Compared with the parental cells, a significant increase in activation of ATM (pS1981),[22] EGFR (pY1068),[23]

FGFR (pY653),[24,25] YAP (pS127),[26] FAK (pY397)[27] and SRC (pY416)[28] was found in IDTCs, all of which have been reported to be potential activators of both ERK and AKT signaling (Figure 6d, Supplementary Table S2). IDTCs also showed an increase in PKCA expression and pS657 phosphorylation, which has been shown to induce AKT and ERK activation[29] and activation of the mTOR pathway, a common downstream target of AKT, ERK and PKCA signaling. Correspondingly, RPPA analyses also showed an increase in RAPTOR and mTOR expression along with an increase in mTOR pS2448 phosphorylation (Figure 6e). Further, as suggested by immunoblotting RPPA analysis also confirmed the upregulation of AKT and ERK phosphorylation along with upregulation of the anti-apoptotic protein BCL-2 (Figure 6f). These results underscore the extent of signaling pathways involved in rendering IDTCs drug tolerant.

IDTCs undergo transition into a permanent drug resistant state under prolonged drug treatment

Reversible drug-induced plasticity has been recently reported followed by the emergence of permanent drug resistance.[3] Hence, we hypothesized that persistent drug exposure would lead to a loss of the transient IDTC state leading to a shift toward a permanent resistant state. WM164 IDTCs were maintained in 500 nM PLX4032 over 90 days and their CD271 expression was monitored on days 12, 23, 58 and 90. Interestingly, the CD271 expression gradually increased from days 12 to 23 but then declined on day 58. After 90 days of continuous drug exposure, the cells completely lost their CD271 expression suggestive of an altered phenotype (Figure 7a). There was also a concomitant decrease in ERK and AKT phosphorylation and JARID1B expression (Figure 7b) along with an increase in cell proliferation (Supplementary Figure S7A). These cells were termed WM164 PLX-R (Resistant). To test whether WM164 PLX-R also account for a nonreversible drug-resistant phenotype and to determine their multidrug-tolerant properties, WM164 PLX-R, IDTCs reversed to the parental state by drug holidays (58 days PLX4032 exposure followed by 45 days drug holiday; 58d IDTC-Rev), and IDTCs were probed for multidrug tolerance by exposing them to PLX4032 (10 μM), GSK1120212 (50 nM), Cisplatin (30 μM), Adrucil (25 μg/ml) and Docetaxel (20 nM). Both the 58d IDTC-Rev and the WM164 PLX-R cells were found to be sensitive to different drugs, suggesting a loss of multidrug tolerance as opposed to IDTCs (Figure 7c). The only difference between WM164 PLX-R and 58d IDTC-Rev cells was their regained sensitivity toward high concentrations of PLX4032 (10 μM). WM164 PLX-R cells displayed no significant increase in caspase 3 activity in contrast to 58d IDTC-Rev cells suggesting that WM164 PLX-R cells exert an acquired drug resistance state toward PLX4032. In addition, a reduced tumorigenic potential for WMM164 PLX-R was also observed in xenografts if compared with WM164 IDTCs, although the cells showed a slightly increased tumor growth than parental cells (data not shown; Figure 7d).

Our results suggest that a profound decrease in CD271 expression under persistent drug exposure characterizes a state of permanent resistance to the specific drug. The reason for this transformation is currently unknown, as a mutational analysis of 409 oncogenes (Ion AmpliSeq Comprehensive Cancer Panel) on parental, IDTCs generated after 58 days and WM164 PLX-R cells did not yield any evidence for de novo mutations to trigger a new phenotype (data not shown). However, rewiring of signaling pathways as a mutation-

independent mechanism leading to permanent resistance has been previously described.[30] Further, we tested whether the WM164 PLX-R cells retained the capacity to exhibit the primary response by exposing the resistant cell populations to a new drug in order to re-induce an IDTC state. WM164 PLX-R cells were exposed to the MEK inhibitor GSK1120212, which caused the re-induction of CD271 (Supplementary Figure S7B), indicative of an IDTC-like phenotype.

DISCUSSION

This study shows that melanoma cells have an innate ability to survive persistent hostile conditions such as drug exposure, hypoxia or nutrient starvation, by exhibiting an early innate response. The primary innate response also induces a multidrug-tolerant state as a primary step preceding acquired drug resistance. The transition from parental cells into IDTCs would provide a buffer period allowing them to accumulate mutations and epigenetic changes for a later permanent gain of drug resistance.

The stress response induces a global chromatin remodeling shifting the cells into a slow cycling state. Loss of H3K4me3 has been reported in a subpopulation of pre-existing cells in the parental population contributing to drug resistance;[4] however, their mode of origin so far is unknown. Our study indicates that the formation of this population could be a direct stress-related response. CD271 expression and the loss of melanoma antigens, another characteristic feature of the IDTC population, leads to resistance in patients subjected to adoptive T-cell transfer therapy suggesting a broader generic mechanism behind this process.[31] Upregulation of CD271 has also been reported to be inducible by interferon γ in melanoma cells.[32] However, forced overexpression of CD271 alone was not sufficient to induce the transition of parental cells while the molecule being still important for the formation of IDTCs as observed in this study. This suggests that IDTC formation could be a product of interrelation between multiple individual components including CD271 upregulation, histone modification and increased activity of multiple signaling pathways.

Accordingly, we observed that the combined strategies including the use of HDAC, IGF1R, Pi3K/AKT inhibitors[4] and oligomycin A targeting mitochondrial survival pathways,[6] along with the primary drug, exert a higher potential to eliminate the parental population before transition into IDTCs, whereas IDTCs by themselves showed an elevated tolerance even toward these combined exposures. The study suggests that multiple factors contribute to the transition and maintenance of the IDTC state and from these observations it is tempting to speculate that the burden of signaling is distributed between multiple pathways unlike the parental BRAF mutant cells, which seem to be primarily dependent on BRAF-driven ERK signaling. Further, persistent drug exposure seems to trigger a transition from IDTCs to a permanently resistant fast-growing cell population, which shows characteristics similar to parental cells, however, being resistant to the drug they were primarily exposed to.

Transposing this concept to the *in vivo* situation would mean that IDTC-like cells are almost certainly present in the tumor because of adverse conditions imposed by the tumor microenvironment and improper drug kinetics. Hence, continuous administration of drugs would inevitably lead to the emergence of multidrug-tolerant IDTCs that upon prolonged

exposure might lead to permanent drug resistance. Employing an intermittent dosing is a timely concept, which has already been shown to delay the emergence of resistance to BRAF inhibitors.[33] This concept needs further investigation along with combination therapies, for example, targeting CD271, KDM5B or HDAC, which might result in a continuous switching between parental and the IDTC state, with each transition gradually reducing the tumor burden thereby leading to chronicity.

MATERIALS AND METHODS

Generation of IDTCs

IDTCs were generated by exposing cancer cells to PLX4032, cisplatin, low glucose or hypoxic conditions for a minimum of 12 days. RPMI media supplemented with 2 mM L-Glutamine, 2 × Penstrep and 5% fetal calf serum were used to maintain the cells. Low-glucose media was made by mixing RPMI normal media in a 1:4 ratio with RPMI media without glucose. Hypoxic experiments were performed in a hypoxic work station facility from Biospherix (Model Nr.: G300CL, BioSpherix, Lacona, NY, USA) at the Ludwig Boltzmann Institute for Lung Vascular Research, Medical University of Graz, Austria. The media were replenished every third day for the period of the experiments.

Gene expression analyses

Gene expression analyses were carried out as previously reported[34] by the Core Facility for Molecular Biology at the Centre of Medical Research at the Medical University of Graz, Graz, Austria. For details please see supplemental methods.

RPPA analysis

Cell lysates were probed with antibodies by a catalyzed signal amplification (CSA) amplification approach and visualized by DAB colorimetric reaction. Slides were scanned and the density was quantified by an Array-Pro Analyzer (TECAN, Maennedorf, Switzerland). For details please see supplementary methods.

Supplementary Material

Refer to Web version on PubMed Central for supplementary material.

ACKNOWLEDGEMENTS

We would like to thank Marcus Absenger (ZMF, Medical University of Graz), Xin Xiao and Palmila Liu (The Wistar Institute, PA, USA) and Maria Grygar (Institute of Pathology, Medical University of Graz, Austria) for technical assistance. This work was supported by the PhD program ‘Molecular Medicine’ of the Medical University of Graz (to DRM and SD) and the Austrian Science foundation (FWF) projects SFB LIPOTOX F30 and W1226 DK “Metabolic and cardiovascular disease” (to GH). We thank Dr Atsushi Miyawaki, RIKEN, Wako-city, Japan, for providing the FUCCI constructs. The FUCCI work was supported by project grants APP1003637 (National Health and Medical Research Council) and RG 09-08 (Cancer Council New South Wales) to NKH.

REFERENCES

1. Flaherty KT, Infante JR, Daud A, Gonzalez R, Kefford RF, Sosman J, et al. Combined BRAF and MEK inhibition in melanoma with BRAF V600 mutations. N Engl J Med. 2012; 367:1694–1703. [PubMed: 23020132]

2. Nazarian R, Shi H, Wang Q, Kong X, Koya RC, Lee H, et al. Melanomas acquire resistance to B-RAF(V600E) inhibition by RTK or N-RAS upregulation. Nature. 2010; 468:973–977. [PubMed: 21107323]

3. Das TM, Salangsang F, Landman AS, Sellers WR, Pryer NK, Levesque MP, et al. Modelling vemurafenib resistance in melanoma reveals a strategy to forestall drug resistance. Nature. 2013; 494:251–255. [PubMed: 23302800]

4. Sharma SV, Lee DY, Li B, Quinlan MP, Takahashi F, Maheswaran S, et al. A chromatin-mediated reversible drug-tolerant state in cancer cell subpopulations. Cell. 2010; 141:69–80. [PubMed: 20371346]

5. Roesch A, Fukunaga-Kalabis M, Schmidt EC, Zabierowski SE, Brafford PA, Vultur A, et al. A temporarily distinct subpopulation of slow-cycling melanoma cells is required for continuous tumor growth. Cell. 2010; 141:583–594. [PubMed: 20478252]

6. Roesch A, Vultur A, Bogeski I, Wang H, Zimmermann KM, Speicher D, et al. Overcoming intrinsic multidrug resistance in melanoma by blocking the mitochondrial respiratory chain of slow-cycling JARID1B(high) cells. Cancer Cell. 2013; 23:811–825. [PubMed: 23764003]

7. Haass NK, Beaumont KA, Hill DS, Anfosso A, Mrass P, Munoz MA, et al. Real-time cell cycle imaging during melanoma growth, invasion, and drug response. Pigment Cell Melanoma Res. 2014; 27:764–776. [PubMed: 24902993]

8. Shakhova O, Sommer L. Testing the cancer stem cell hypothesis in melanoma: the clinics will tell. Cancer Lett. 2013; 338:74–81. [PubMed: 23073475]

9. Tiwari N, Tiwari VK, Waldmeier L, Balwierz PJ, Arnold P, Pachkov M, et al. Sox4 is a master regulator of epithelial-mesenchymal transition by controlling Ezh2 expression and epigenetic reprogramming. Cancer Cell. 2013; 23:768–783. [PubMed: 23764001]

10. Frank NY, Margaryan A, Huang Y, Schatton T, Waaga-Gasser AM, Gasser M, et al. ABCB5-mediated doxorubicin transport and chemoresistance in human malignant melanoma. Cancer Res. 2005; 65:4320–4333. [PubMed: 15899824]

11. Alla V, Kowtharapu BS, Engelmann D, Emmrich S, Schmitz U, Steder M, et al. E2F1 confers anticancer drug resistance by targeting ABC transporter family members and Bcl-2 via the p73/DNp73-miR-205 circuitry. Cell Cycle. 2012; 11:3067–3078. [PubMed: 22871739]

12. Elliott AM, Al-Hajj MA. ABCB8 mediates doxorubicin resistance in melanoma cells by protecting the mitochondrial genome. Mol Cancer Res. 2009; 7:79–87. [PubMed: 19147539]

13. Duan Z, Brakora KA, Seiden MV. Inhibition of ABCB1 (MDR1) and ABCB4 (MDR3) expression by small interfering RNA and reversal of paclitaxel resistance in human ovarian cancer cells. Mol Cancer Ther. 2004; 3:833–838. [PubMed: 15252144]

14. Chen YT, Stockert E, Jungbluth A, Tsang S, Coplan KA, Scanlan MJ, et al. Serological analysis of Melan-A(MART-1), a melanocyte-specific protein homogeneously expressed in human melanomas. Proc Natl Acad Sci USA. 1996; 93:5915–5919. [PubMed: 8650193]

15. Kwon BS. Pigmentation genes: the tyrosinase gene family and the pmel 17 gene family. J Invest Dermatol. 1993; 100(2 Suppl):134S–140S. [PubMed: 8432998]

16. Moreb JS. Aldehyde dehydrogenase as a marker for stem cells. Curr Stem Cell Res Ther. 2008; 3:237–246. [PubMed: 19075754]

17. Raha D, Wilson TR, Peng J, Peterson D, Yue P, Evangelista M, et al. The cancer stem cell marker aldehyde dehydrogenase is required to maintain a drug-tolerant tumor cell subpopulation. Cancer Res. 2014; 74:3579–3590. [PubMed: 24812274]

18. Koch CM, Andrews RM, Flicek P, Dillon SC, Karaöz U, Clelland GK, et al. The landscape of histone modifications across 1% of the human genome in five human cell lines. Genome Res. 2007; 17:691–707. [PubMed: 17567990]

19. Barski A, Cuddapah S, Cui K, Roh TY, Schones DE, Wang Z, et al. High-resolution profiling of histone methylations in the human genome. Cell. 2007; 129:823–837. [PubMed: 17512414]

20. Poulikakos PI, Rosen N. Mutant BRAF melanomas--dependence and resistance. Cancer Cell. 2011; 19:11–15. [PubMed: 21251612]

21. Huang PH, Chen CH, Chou CC, Sargeant AM, Kulp SK, Teng CM, et al. Histone deacetylase inhibitors stimulate histone H3 lysine 4 methylation in part via transcriptional repression of histone H3 lysine 4 demethylases. Mol Pharmacol. 2011; 79:197–206. [PubMed: 20959362]

22. Khalil A, Morgan RN, Adams BR, Golding SE, Dever SM, Rosenberg E, et al. ATM-dependent ERK signaling via AKT in response to DNA double-strand breaks. Cell Cycle. 2011; 10:481–491. [PubMed: 21263216]
23. Grant S, Qiao L, Dent P. Roles of ERBB family receptor tyrosine kinases, and downstream signaling pathways, in the control of cell growth and survival. Front Biosci. 2002; 7:d376–d389. [PubMed: 11815285]
24. Mohammadi M, Dikic I, Sorokin A, Burgess WH, Jaye M, Schlessinger J. Identification of six novel autophosphorylation sites on fibroblast growth factor receptor 1 and elucidation of their importance in receptor activation and signal transduction. Mol Cell Biol. 1996; 16:977–989. [PubMed: 8622701]
25. Zou L, Cao S, Kang N, Huebert RC, Shah VH. Fibronectin induces endothelial cell migration through beta1 integrin and Src-dependent phosphorylation of fibro-blast growth factor receptor-1 at tyrosines 653/654 and 766. J Biol Chem. 2012; 287:7190–7202. [PubMed: 22247553]
26. Overholtzer M, Zhang J, Smolen GA, Muir B, Li W, Sgroi DC, et al. Transforming properties of YAP, a candidate oncogene on the chromosome 11q22 amplicon. Proc Natl Acad Sci USA. 2006; 103:12405–12410. [PubMed: 16894141]
27. Glover S, Delaney M, Dematte C, Kornberg L, Frasco M, Tran-Son-Tay R, et al. Phosphorylation of focal adhesion kinase tyrosine 397 critically mediates gastrin-releasing peptide's morphogenic properties. J Cell Physiol. 2004; 199:77–88. [PubMed: 14978737]
28. Kim LC, Song L, Haura EB. Src kinases as therapeutic targets for cancer. Nat Rev Clin Oncol. 2009; 6:587–595. [PubMed: 19787002]
29. Haughian JM, Reno EM, Thorne AM, Bradford AP. Protein kinase C alpha-dependent signaling mediates endometrial cancer cell growth and tumorigenesis. Int J Cancer. 2009; 125:2556–2564. [PubMed: 19672862]
30. Villanueva J, Vultur A, Lee JT, Somasundaram R, Fukunaga-Kalabis M, Cipolla AK, et al. Acquired resistance to BRAF inhibitors mediated by a RAF kinase switch in melanoma can be overcome by cotargeting MEK and IGF-1R/PI3K. Cancer Cell. 2010; 18:683–695. [PubMed: 21156289]
31. Landsberg J, Kohlmeyer J, Renn M, Bald T, Rogava M, Cron M, et al. Melanomas resist T-cell therapy through inflammation-induced reversible dedifferentiation. Nature. 2012; 490:412–416. [PubMed: 23051752]
32. Furuta J, Inozume T, Harada K, Shimada S. CD271 on melanoma cell is an IFN-gamma-inducible immunosuppressive factor that mediates downregulation of melanoma antigens. J Invest Dermatol. 2014; 134:1369–1377. [PubMed: 24226422]
33. Das TM, Stuart DD. The evolution of melanoma resistance reveals therapeutic opportunities. Cancer Res. 2013; 73:6106–6110. [PubMed: 24097822]
34. Cvitic S, Longtine MS, Hackl H, Wagner K, Nelson MD, Desoye G, Hiden U. The human placental sexome differs between trophoblast epithelium and villous vessel endothelium. PloS one. 2013; 8:e79233. [PubMed: 24205377]

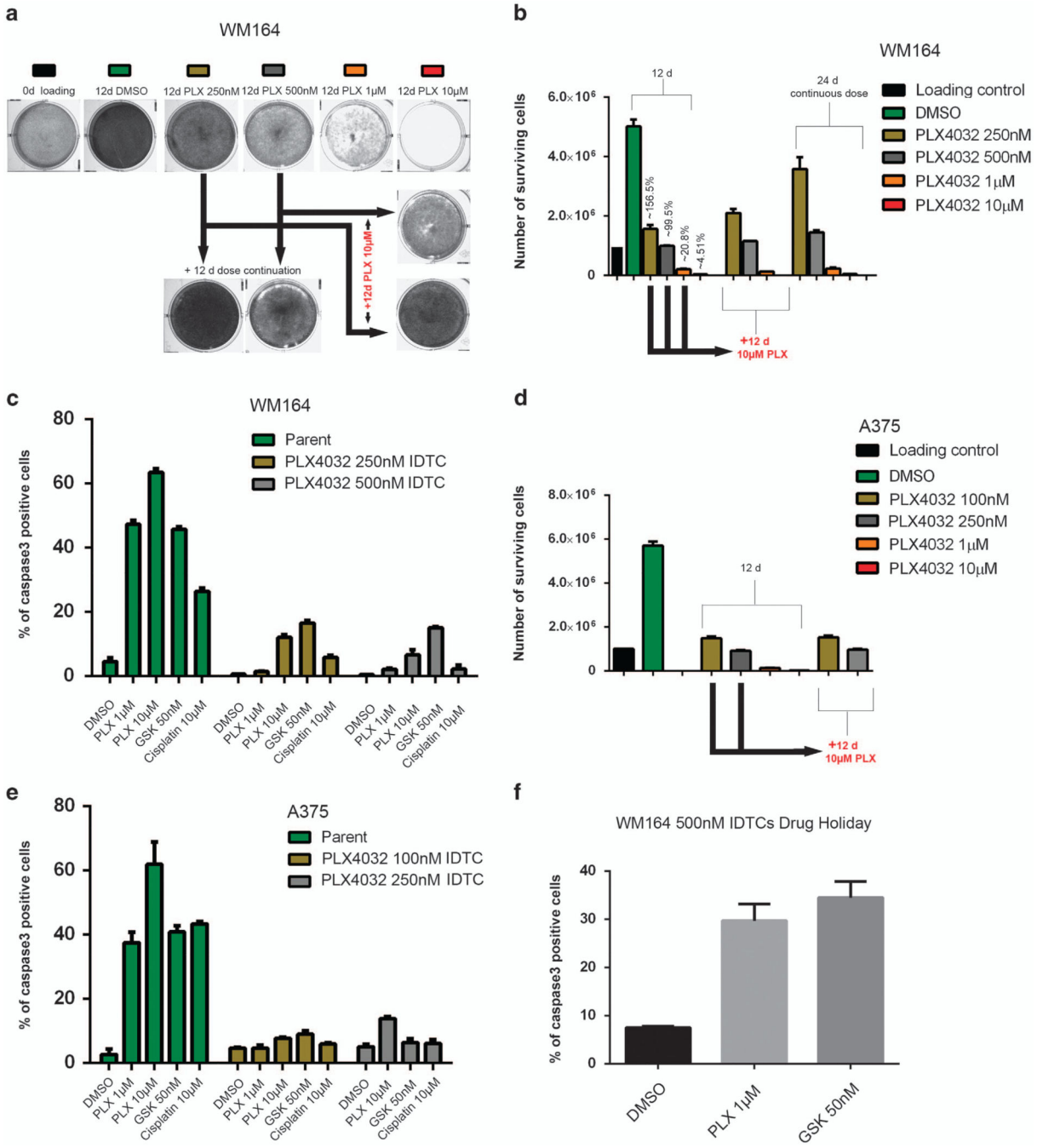

Figure 1.

An early innate response leads to multidrug tolerance in BRAF-mutated melanoma cells. In all, 1×10^6 WM164 cells were plated in triplicate for each time point and drug concentration, and exposed to dimethyl sulphoxide (DMSO) or PLX4032 (250 nM, 500 nM, 1 and 10 μM) for 12 days. One of the three triplicates was subjected to crystal violet staining as a representative image (**a**). The number of viable cells was counted from two experimental duplicates and depicted as bar graphs. Error bars represent the s.d. from the mean (**b**). Cells exposed to 250 and 500 nM of PLX4032 were further subjected to 10 μM of PLX4032 for

another 12 days. WM164 was separately continuously exposed to 250 and 500 nM of PLX4032 for 24 days as an internal control to understand the growth dynamics for each concentration. After 24 days one of the triplicates was stained with crystal violet (**a**) and the number of viable cells was analyzed by cell counting (**b**). Error bars represent the s.d. from the mean. (**c**) WM164 PLX4032 250 and 500 nM IDTCs (WM164 250 nM IDTC, WM164 500 nM IDTC) were exposed to PLX4032 at 1 or 10 μM, GSK1120212 at 50 nM and cisplatin at 30 μM for 48 h and cells were analyzed by flow cytometry for the percentage of caspase 3-positive cells. Error bars represent the s.d. from the mean. Twenty-four days' experiments as in **a**, **b** were repeated in A375 cells with PLX4032 at 100 nM, 250 nM, 1 and 10 μM. The viable cells were counted and depicted as bar graphs. Error bars represent the s.d. from the mean (**d**). A375 PLX4032 100 and 250 nM IDTCs were subjected to PLX4032 at 1 or 10 μM, GSK1120212 at 50 nM and cisplatin at 30 μM for 48 h and cells were analyzed by flow cytometry for activated caspase 3. Error bars represent the s.d. from the mean (**e**). (**f**) WM164 500 nM IDTCs were allowed a 7-day drug holiday and, subsequently, were subjected to 1 and 10 μM of PLX4032. The percentage of caspase 3-positive cells was analyzed by flow cytometry. Error bars represent the s.d. from the mean.

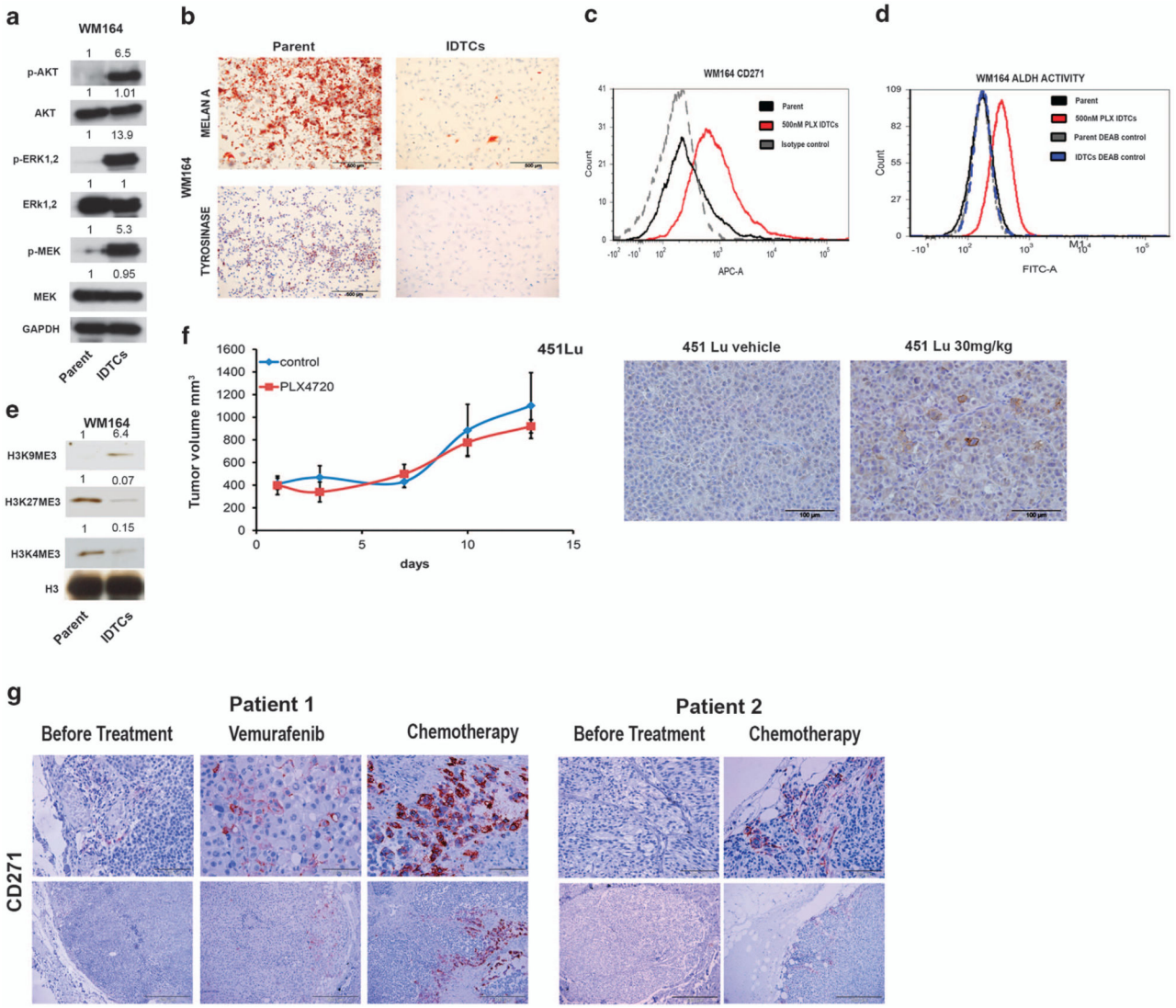

Figure 2.

Common features of IDTCs. (**a**) Protein lysates of WM164 500 nM IDTCs and parental cells were subjected to immunoblotting for expression levels of phosphorylated ERK1,2 (p-ERK1,2 {Thr202/Tyr204}), total ERK (T-ERK1,2), phosphorylated MEK1,2 (p-MEK {Ser217/221}), total MEK1,2 (T-MEK), phosphorylated AKT (p-AKT {Ser473}), total AKT (T-AKT) and band intensities were quantified taking GAPDH as loading control. (**b**) Positive staining of Melan A and tyrosinase was analyzed in WM164 parent and IDTCs by immunocytochemistry. WM164 parental and WM164 500 nM PLX IDTCs (red) were subjected to flow cytometry to determine CD271 expression (**c**) and ALDH activity (**d**) with their respective isotype and diethylamino benzaldehyde (DEAB)-negative controls. (**e**) Histones were isolated in total from parental (parent) and WM164 IDTCs (IDTCs) and immunoblotting was performed with H3, H3K4me3, H3K9me3 and H3K27me3 antibodies. Band intensities were quantified with H3 as loading control. (**f**) Human melanoma cells (451Lu) xenografted to NOD SCID interleukin 2 receptor gamma chain knockout mice (five per group) treated with mock (451Lu DMSO) or 30 mg/kg/day PLX4720 for 2 weeks

(451Lu 30 mg/kg). Tumor volume measured twice weekly (left). After 2 weeks, tumors were isolated and analyzed for CD271 expression by immunohistochemistry (right). (**g**) (Patient 1) Tissue slides prepared from biopsies of subcutaneous metastases of a melanoma patient stained for CD271 before treatment, after 8 months of treatment with Vemurafenib and after 2 months of treatment with taxol and cisplatin. (Patient 2) Biopsies from subcutaneous metastases of a patient, before treatment (left) in comparison with 1 month after initiation of treatment with dacarbazine (right).

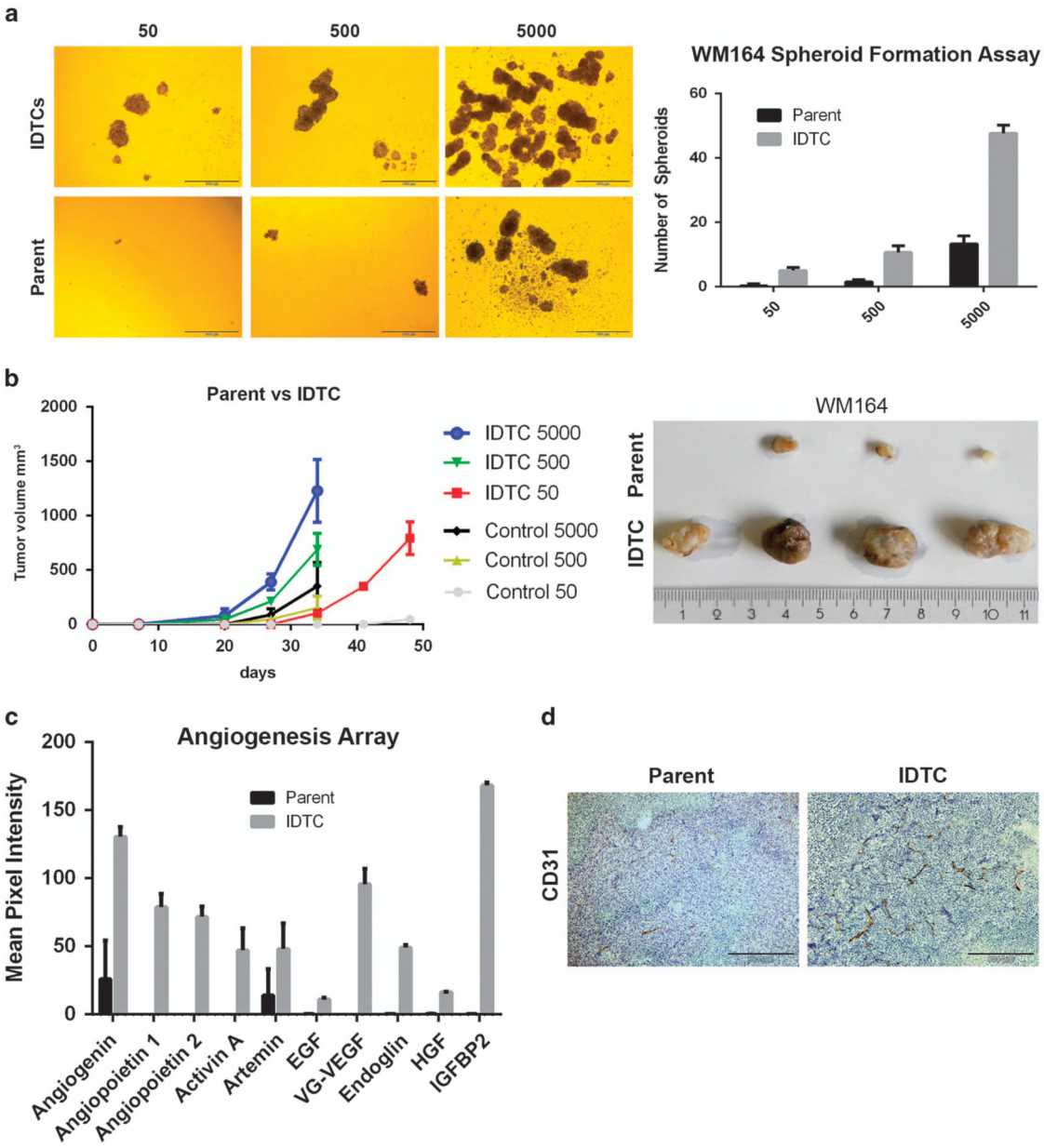

Figure 3.

Sphere-forming capacity and tumorigenicity of IDTCs. (**a**) Representative pictures of WM164 parental and 500 nM IDTC spheres plated at 50, 500 and 5000 cells per well after 7 days (left). Experiments were carried out in triplicate and the number of spheres per well was quantified and represented as bar graphs (right). (**b**) Tumor volume after subcutaneous injection into NOD.CB17-Prkdcscid/J mice of WM164 parental or 500 nM IDTCs (15 days treatment) at 50 (*n* = 4), 500 (*n* = 4) or 5000 (*n* = 5; left). (Right) Representative pictures of WM164 parent and IDTC tumors generated out of the 50 cells after 7 weeks. (**c**) The mean pixel intensity of the angiogenic cytokine and growth factor profile from conditioned medium of WM164 parental and IDTCs as determined by an angiogenesis array. Data were analyzed by the Image J background subtraction method and plotted as bar graphs. Error

bars represent the s.d. from the mean. Statistical analysis was carried out using two-way analysis of variance and column factor P-value (Parent vs IDTCs) was observed to be 0.0001, suggesting significant difference. (**d**) CD31 expression from WM164 IDTC tumors (500 group) and parental tumors (500 group) by subjecting fixed tissue to immunohistochemistry analysis.

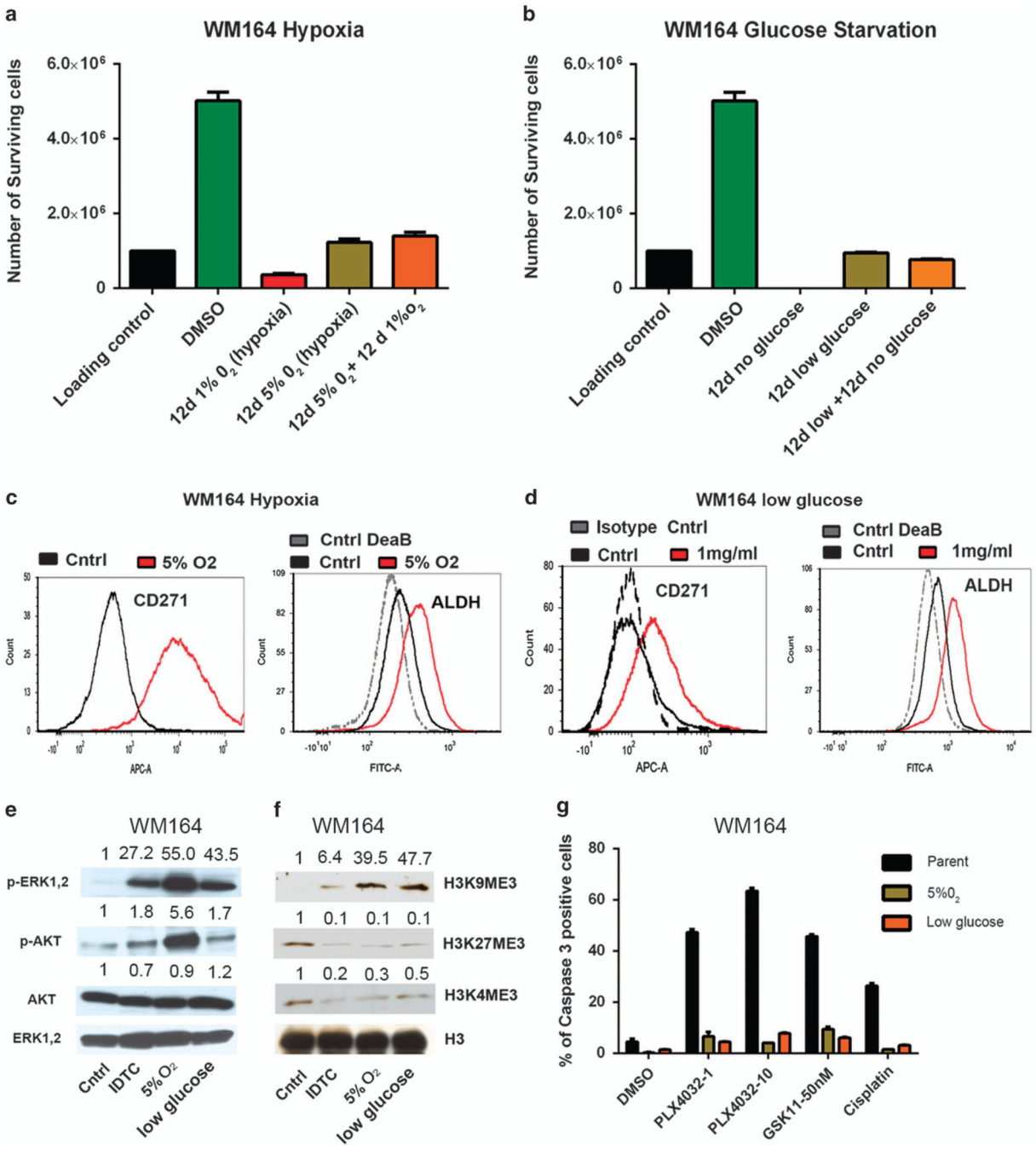

Figure 4.

Hypoxic and low-glucose conditions lead to IDTC-like cells. (**a**) 1×10^6 WM164 cells were subjected to 5% O_2 or 1% O_2 hypoxic conditions for a period of 12 days and the number of viable cells was counted. They were further exposed for 12 days to 5% O_2 and to 1% O_2 for another 12 days and the number of viable cells was counted. The error bars represent s.d.'s from the mean. (**b**) The same as in a, but under low-glucose conditions. WM164 cells were exposed to no glucose or low glucose (1 mg/ml) media for a period of 12 days and the number of viable cells was counted. Cells exposed to low glucose were subjected to no

glucose media for another 12 days and the number of viable cells was counted and plotted as a graph. The error bars represent the s.d. from the mean. WM164 parental cells, cells exposed to 5% O_2 (**c**) and low glucose (**d**) for 12 days, were analyzed for their CD271 and ALDH activity by flow cytometry. (**e**) Lysates of WM164 500 IDTCs, parental cells and cells exposed to 12 days of hypoxia or low glucose were subjected to immunoblotting to detect phosphorylated ERK1,2 (p-ERK1,2(Thr202/ Tyr204)), total ERK (T-ERK1,2)), phosphorylated AKT (p-AKT (Ser473)) and total AKT (T-AKT). Band intensities were quantified with ERK1,2 as loading control. (**f**) Histone was isolated from parental and WM164 IDTC cells exposed to 12 days of hypoxia or low glucose, and subjected to immunoblotting with H3, H3K4me3, H3K9me3 and H3K27me3 antibodies. Band intensities were quantified with H3 as the loading control (the blots are in part presented in Figure 2e). (**g**) WM164 cells exposed to 12 days of hypoxia or low glucose were challenged with PLX4032 at 1 and 10 μM, GSK1120212 50 nM and cisplatin at 10 μM for 48 h, and the percentage of caspase 3-positive cells was analyzed by flow cytometry and compared with the parental population. Error bars represent the s.d. from the mean.

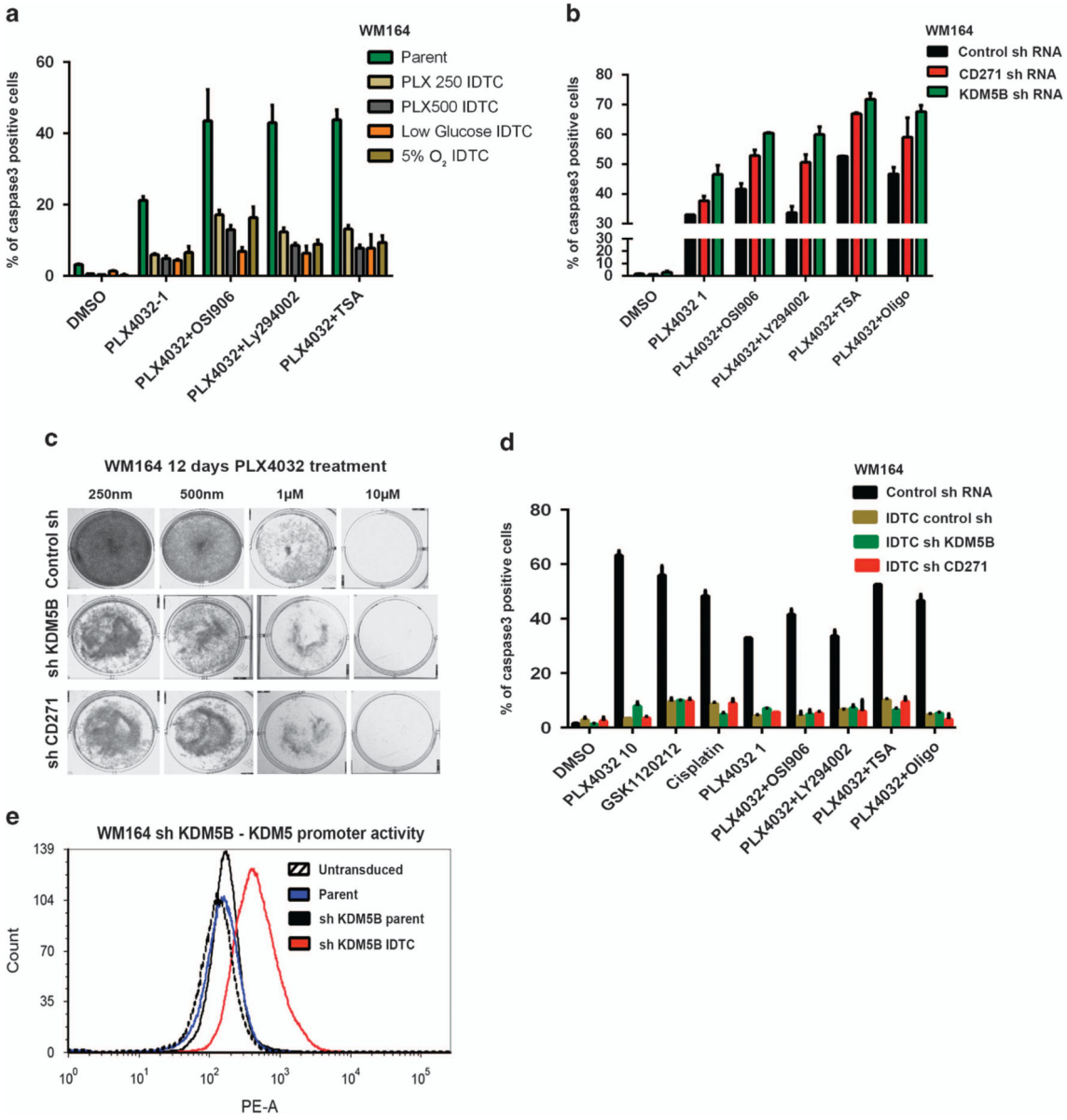

Figure 5.

Knockdown of CD271 or KDM5B sensitizes parental cells to single or combined drug exposures but the emerging IDTCs again show multidrug tolerance. (**a**) WM164 parental, PLX4032 250 nM IDTCs (PLX 250 IDTC), PLX4032 500 nM IDTCs (PLX 500 IDTC), low-glucose IDTCs (low-glucose IDTC) and 5% O_2 induced IDTCs (5% hypoxia IDTC) were exposed to either DMSO or PLX4032 alone (1 v) or PLX4032 (1 μM) in combination with one of the following inhibitors OSI906 (5 μM), Ly294002 (10 μM) or TSA (100 nM) for a period of 36 h and active caspase 3 expression in cells was analyzed by flow cytometry. Error bars represent the s.d. from the mean. (**b**) WM164 control shRNA-transduced, shCD271 RNA-transduced (red) and shKDM5B RNA-transduced cells were exposed to PLX4032 (1 μM) or in combination with one of the following inhibitors OSI906 (5 μM), Ly294002 (10 μM), TSA (100 nM) or Oligomycin A (1 μg/ml) and the percentage of caspase

3-positive cells depicted as bar graphs. Error bars represent the s.d. from the mean. (**c**) WM164 control shRNA-transduced, shCD271 RNA-transduced and shKDM5B RNA-transduced cells were exposed to PLX4032 250 nM, 500 nM, 1 or 10 μM for a period of 12 days and the residual surviving cells were stained with crystal violet. (**d**) WM164 control shRNA-transduced, control shRNA-transduced IDTCs, shCD271 RNA-transduced IDTCs and shKDM5B RNA-transduced IDTCs were exposed to GSK1120212 (50 nM), cisplatin (30 μM), PLX4032 (10 μM), PLX4032 (1 μM) and PLX4032 (1 μM) in combination with one of the following inhibitors OSI906 (5 μM), Ly294002 (10 μM), TSA (100 nM) or Oligomycin A (1 μg/ml) for 48 h and the percentage of caspase 3-positive cells was analyzed by flow cytometry. Error bars represent the s.d. from the mean. (**e**) WM164 shKDM5B-transduced cells were transduced with a Ds red KDM5 promoter (shKDM5 parental (black)) and transformed into the IDTC state by exposure to 250 nM PLX4032 for 12 days (shKDM5 IDTC (red)). Their KDM5 activity was analyzed by flow cytometry and compared with the WM164 parent KDM5 promoter-transduced cells (parental (blue)) and WM164 parent-non-transduced cells (untransduced).

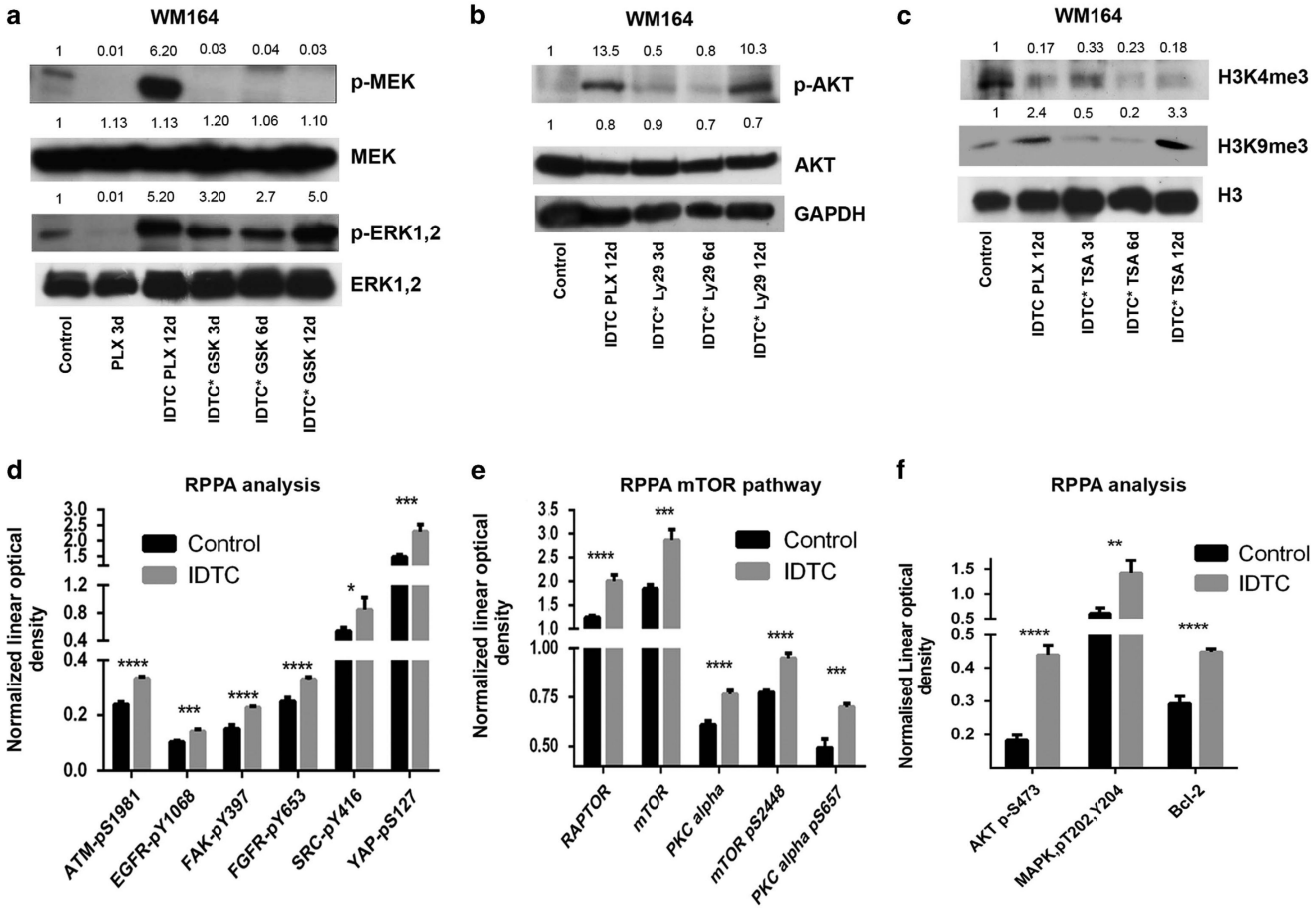

Figure 6.

Rewiring of signaling in IDTCs to targeted inhibitors. (**a**) Immunoblot of WM164 parent (control (DMSO), PLX 3d (PLX4032 3 days)) and WM164 PLX4032 IDTCs (IDTC PLX 12d) for phosphorylated ERK1,2 (p-ERK1,2(Thr202/Tyr204)), total ERK (T-ERK1,2), phosphorylated MEK1,2 (p-MEK Ser217/221) and total MEK1,2 (T-MEK) if exposed to either PLX4032 (1 μM) alone or in combination (*) with GSK1120212 (50 nM) at various time points (0, 3, 6 and 12 days). Band intensities were quantified with ERK as loading control. (**b**) Immunoblot of WM164 parental (control (DMSO)) and WM164 IDTCs for phosphorylated AKT (p-AKT (Ser473)), total AKT (T-AKT) and GAPDH when exposed to PLX4032(1 v) alone or in combination (*) with LY294002 (10 μM) at various time points (0, 3, 6 and 12 days). Band intensities were quantified with GAPDH as loading control. (**c**) Immunoblot of WM164 parental (control (DMSO)) and WM164 IDTCs for H3, H3K4me3, H3K9me3 if exposed to PLX4032 (1 μM) alone or in combination (*) with TSA (100 nM) at various time points (0, 3, 6 and 12 days). Band intensities were quantified with H3 as loading control. (**d**–**f**) RPPA analyses depicted as the normalized linear optical density of proteins in WM164 parental and IDTCs (gray) lysates. Error bars represent the s.d. from the mean. Statistical analysis was carried out using the t-test and the P-value is represented by (*), where ****$P \leq 0.0001$, ***$P \leq 0.001$, **$P \leq 0.01$ and *$P \leq 0.05$.

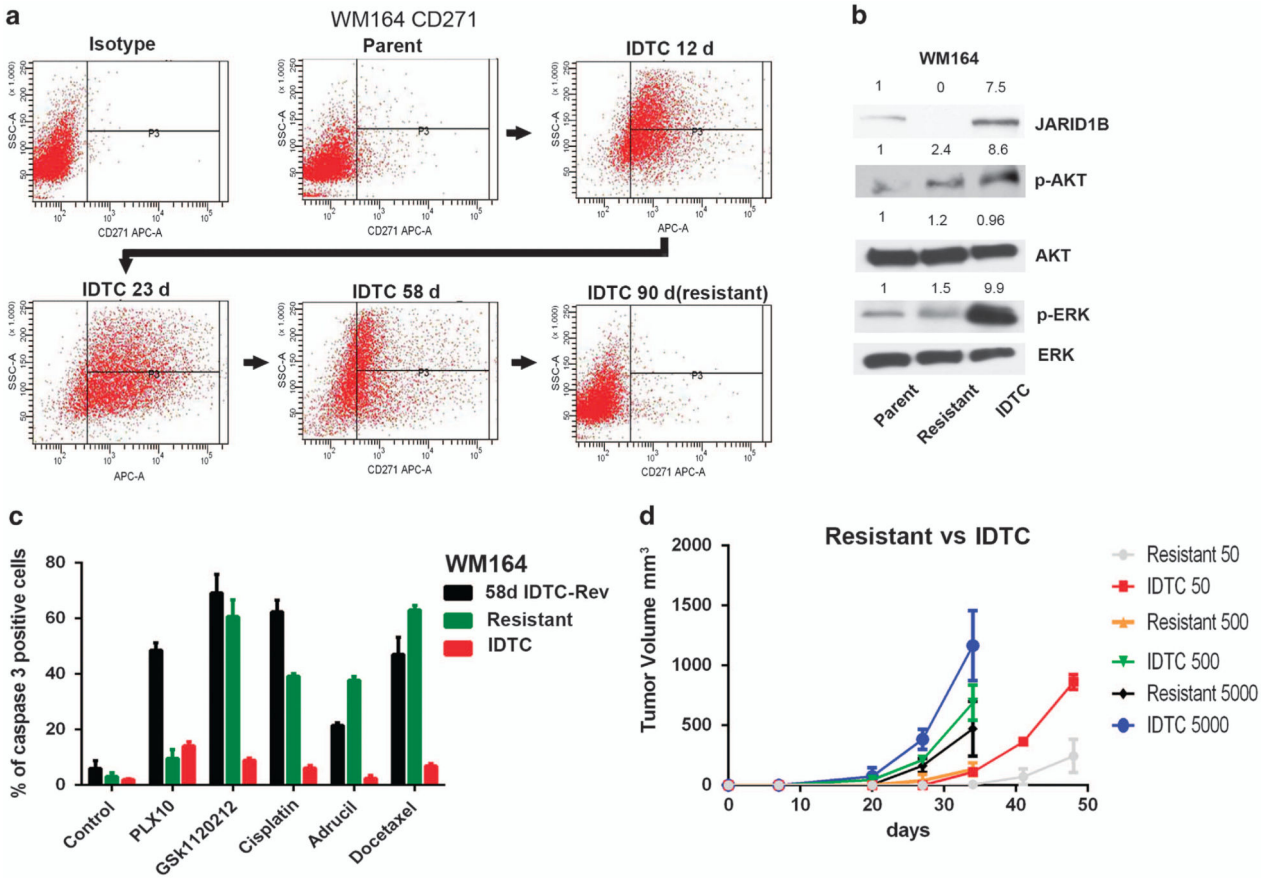

Figure 7.

IDTCs transform into a permanent drug-resistant state under persistent drug exposure. (**a**) CD271 expression of WM164 cells exposed to 500 nM of PLX4032 during different time points over 90 days analyzed by flow cytometry. (**b**) Immunoblot of WM164 parental, resistant (WM164 cells exposed to 500 nM PLX4032 for 90 days) and IDTCs for KDM5B, phosphorylated AKT (p-AKT (Ser473)), total AKT (T-AKT), phosphorylated ERK1,2 (p-ERK1,2 (Thr202/Tyr204)), total ERK (T-ERK1,2). Band intensities were quantified with total ERK as loading control. (**c**) WM164 58d IDTC-Rev, WM164-resistant (Resistant) and WM164 IDTCs (40-day old; IDTC) exposed to PLX4032 at 10 μM (PLX10), GSK1120212 (50 nM), cisplatin (30 μM), Adrucil (25 μg/ml) and docetaxel (20 nM) for 48 h and the percentage of caspase 3-positive cells was analyzed by flow cytometry. Error bars represent the s.d. from the mean. (**d**) Tumor volume after subcutaneous injection into NOD.CB17-Prkdcscid/J mice at 50 (n = 3), 500(n = 4) or 5000(n = 4) cells of WM164-resistant or 500 nM IDTC cells. The tumor volume was measured at indicated time points.